Experimental determination of the mechanical behavior of Compacted exfoliated vermiculite

Soufiane Belhouideg , Manuel Lagache

Abstract— A series of compacted exfoliated vermiculite (CEV) samples were prepared and their mechanical behavior was experimentally studied. The vermiculite was first exfoliated and after compacted in order to obtain a material with good thermal and mechanical properties. The as-prepared samples have been tested under compressive loading. Some parameters effect was studied, as the porosity and the type of the CEV. The samples of this porous media display two steps for the stress–strain behavior under uniaxial compressive loading, i.e., initial nonlinear deformation, strain-hardening 'pseudo-platform' stage**.**

   Keywords—porous media, compression test, clay, mechanical behavior

I. INTRODUCTION

IN recent years, argillaceous material have spurred considerable interest in the sealing industry [1-3]. Partly because of their potential for large range of temperature and pressures uses compared to standard sealing structures, as elastomers. Vermiculite represents an interesting alternative to asbestos and to exfoliated graphite for high temperature sealing applications. Indeed, because of its chemical and thermal stability, many applications, as high temperatures and high pressures sealing, are possible. The vermiculite material is a hydrated magnesium aluminum silicate. This media has an clay structure made by the stacking of two types of flakes. Moreover, the vermiculite could be subjected to thermal or chemical exfoliation to obtain expanded material. From the compaction of exfoliated vermiculite, it could result a porous material with very low permeability, good mechanical properties, chemical and thermal stability.

The elastic constants (e.g., Young's modulus, shear modulus) are among the basic mechanical properties of a material that control the essential small strain behaviour, a material's response to force at the elastic regime.

Recently clays or other layered hydrous aluminosilicates have been used to make clay–polymer nanocomposites and clay-based nanostructured multilayers [4-6]. Modeling and understanding the behavior of manufactured clay-based nanocomposites require the understanding of the fundamental elastic properties and hardness of the filling clay minerals [7]. The purpose of this paper is to study the mechanical behavior of CEV and the effect of some parameters as type of CEV. The first part of this series is devoted to a general presentation of the materials which have been used and the elaboration of the CEV samples. The microstructure of the CEV was identified by using scanning electron microscopy (SEM). A reminder of the poromechanical behavior is exposed. Finally, the procedure of compression test is presented. Results of systematic measurements of mechanical properties are gathered in second section.

II. EXPERIMENTAL PROCEDURES

A. Preparation process

The vermiculite used in this study is exfoliated vermiculite Granutech E from China (Yuli), distributed by the Comptoir des Minéraux et de Matières Premières de Paris *(CMMP)*. The mean size of these vermiculite particles is in the range of 0.7 to 2 mm. In order to reduce the size of these particles, different treatments were tested [8]. The ultrasonic irradiation in H_2O_2 (hydrogen peroxide) leads to reduce the particle size. So, for treatment of acceptable time (5h), the measured average particle size is about 2.0 µm [8]. It is important to underline that the particle size of vermiculite, used in this study, is very different from the size of the vermiculite particles commonly encountered.

To manufacture samples of compacted exfoliated vermiculite, a metal mold with cylindrical shape was used. Several types of samples were prepared by pressing the powder of vermiculite at room temperature (20 °C) and 200 °C (up to 4 °C/min). Three kinds of samples were elaborated:

  - Vermiculite powder exchanged with potassium (K^+) [8]. The compaction temperature is T = 200 °C. The reference used is VK200.
  - Vermiculite powder exchanged with potassium (K^+) [8]. The compaction temperature is T = 20 °C. The reference used is VK20.
  - Vermiculite powder exchanged with lithium (Li^+) [8]. The compaction temperature is T = 20 °C. The reference used is VL20.

The vermiculite powder was put into a cylindrical mold. The powder was compacted by a moving piston with a controlled pressure (Fig. 1). The pressure applied with the piston was about 80 MPa. The temperature could be fixed during the

   S. Belhouideg and M. Lagache are with Laboratoire SYMME, Université de Savoie, BP 80439 F74944 Annecy le Vieux Cedex , France (corresponding author: S. Belhouideg; : +33 479 758 132; Fax: +33 450 096 543; soufianebelhouideg@ gmail.com).

holding pressure time. Different compaction pressures and different temperatures (20 °C and 200 °C) of implementation were used to study the influence of these parameters on the mechanical properties of CEV.
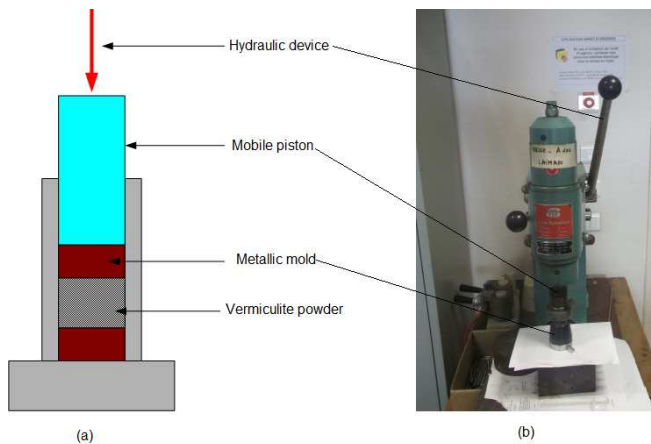

Fig. 1 Preparation process of the CEV samples: (a) schematic of the implementation tool (b) picture of the implementation tool

- Protocol at room temperature

To obtain cylindrical samples with a diameter of 8 or 13 mm and a height about 4 mm (Fig. 2), a quantity of exfoliated vermiculite powder was compacted at desired pressure and at room temperature during 30 min. The quantity of vermiculite required depends on the kind of powder and the size of the mold, as shown in Table 1.

	Mold diameter: 8 mm. Sample height: 3.85±0.18 mm	Mold diameter: 13 mm. Sample height: 3.85±0.18 mm
VK	390 mg	1000 mg
VL	490 mg	1260 mg

Table 1 Quantity of powder required to elaborate samples

- Protocol at 200°C

The protocol of implementation was identical to the previous with a temperature of 200 °C and a compaction time of 3 h. After stabilizing the pressure for 15 minutes at 80 MPa, the mold is heated (up to 4 °C / min) to reach the temperature of 200 °C during 45 min. After 2 h at 200 °C with a pressure of 80 MPa, the pressure was released and the mold was cooled at ambient air during 1 h.

Fig. 2 CEV sample

B. Micro-structure analysis

Experimental techniques, most commonly used to characterize a porous media, are: mercury porosimetry, scanning electron microscopy and micro-tomography…

Each of these techniques contributes to the knowledge of a precise part of the micro geometry: porosity volume fraction, specific surface, pore size distribution… Among these techniques, mercury porosimetry is the technique most used to characterize a porous material. This experimental measure provides the porosity volume ratio, the pore size distribution...of connected porosities [9]. This technique is based on measuring of the quantity of mercury at different pressures (mercury intrusion).

On the other hand, scanning electron microscopy (SEM) has a destructive character due to the problem of sample preparation. The sample needs to be dried, polished and metalized or cut into thin sections. Despite these disadvantages, this experimental technique provides easily information on the micro scale. The SEM gives an idea about the microstructure of porous media, but it does not generally provide direct three-dimensional information.

Also, the micro-tomography allows to obtain a 3D image of a scanned sample. This technique is based on the multi-directional analysis of the interaction between a X-rays beam and the material [10]. Structural properties such as the porosity, specific surface area, pore-size distribution and local geometry distribution of the sample are directly extracted from the tomographic data. However, the need for high resolution (due to the small pores size) raises important difficulties for the studied material. Reliable discrimination of pore and solid phases was expected to be limited by the X-ray tube's focal spot size. The voxel size was generally greater than 0.8 μm (obtained using nano-focus CT) [11] and therefore the geometries of sizes of the studied media cannot be characterized with this experimental technique

In order to study the microstructure (layout of vermiculite flakes, porosity ...) of the CEV samples, a scanning electronic microscope LEO 440 Stereoscan with a tungsten filament was used. The observations were made on the lateral side of cylindrical samples and on samples with a flat surface, cut with a microtome Leica RM2165, as shown in Fig. 3. Six parallelepiped samples (4mm× 5mm×4mm) were analyzed. The large size of sample allows to do several observations in different areas in order to obtain representative average information on CEV (Fig. 3).

Pores appear as dark areas allowing to distinguish and quantify them by image analysis. The pores were identified by thresholding of the pore brightness to produce a binary image [12]. The dark area fraction was evaluated and the pore volume ratio was determined. Moreover, the image analysis allows to estimate the angular distribution of porosities.
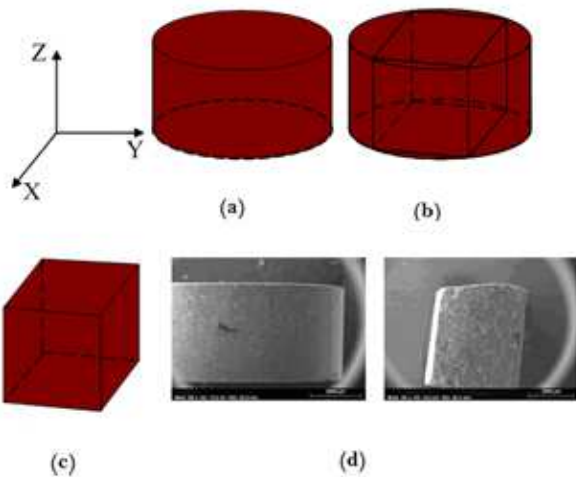
Fig. 3 Sample used for observation by SEM: (a) cylindrical sample (b) cutting plane (c) parallelepiped sample (d) CEV sample

C. Poro-elastic behavior

The study of the mechanical behavior of the porous media was formalized in the 1930's with the works of Terzaghi [13]. Then some developments were proposed by Biot [14] with the first general formulation of the reversible behavior of the porous media. The Biot's theory supposes that the medium consists of two phases: a solid phase (matrix) and a porous phase saturated by a fluid. The behavior of porous media depends on the behavior of each phase, the pressure of the interstitial fluid and the exchanges or non-exchanges of fluid with outside. There are two cases:

a- The drained configuration (fluid exchange with outside), the pressure remains constant inside the porous media.

b- The no drained configuration. There are no fluid exchanges with outside.

The linear poroelastic law has the following form:

$$\begin{cases} \underline{\underline{\sigma}} = \underline{\underline{C}} : \underline{\underline{\varepsilon}} - M.\underline{\underline{B}}.\dfrac{m}{\rho_0^f} & \text{(no drained configuration)} \\[2ex] \underline{\underline{\sigma}} = \underline{\underline{C}}_0 : \underline{\underline{\varepsilon}} - \underline{\underline{B}}.p & \text{(drained configuration)} \end{cases} \quad (1)$$

$\underline{\underline{\sigma}}$: Stress tensor, $\underline{\underline{C}}$: No drained rigidity tensor, $\underline{\underline{C}}_0$: Drained rigidity tensor, $\underline{\underline{\varepsilon}}$: Strain tensor, M : Biot coefficient, $\underline{\underline{B}}$: Biot tensor, m : fluid mass supply per unit of initial volume, p : interstitial pressure and ρ_0^f: Fluid density at initial configuration.

Vermiculite, matrix of studied porous media, is anisotropic and it could to be considered as transverse isotropic [15, 16]. Indeed, the matrix issues from the compression of sheets vermiculite clusters. Due to the preferred orientation of these sheets perpendicular to the compaction axis (SEM observation), the assumption of transverse isotropy seems justified. The vermiculite flakes are predominantly perpendicularly to the axis of compaction. For a transverse isotropic material, only five independent elastic constants are needed to describe the elastic behavior. If the axis of isotropy is the axis 3 (compaction axis) (Fig. 4), the independent elastic parameters are: two Young modulus (E_1 and E_3), two Poisson's coefficients (ν_{12} and ν_{13}) and shear modulus (G_{13}). The following relationships must be satisfied:

$$G_{12} = \frac{E_1}{2(1+\nu_{12})} \quad (2)$$

$$\frac{\nu_{13}}{E_1} = \frac{\nu_{31}}{E_3} \quad (3)$$

The compliance matrix can be written as follows (formula (4)) (Voigt's notation):

$$S = \begin{pmatrix} \dfrac{1}{E_1} & \dfrac{-\nu_{12}}{E_1} & \dfrac{-\nu_{13}}{E_1} & 0 & 0 & 0 \\[2ex] \dfrac{-\nu_{12}}{E_1} & \dfrac{1}{E_1} & \dfrac{-\nu_{13}}{E_1} & 0 & 0 & 0 \\[2ex] \dfrac{-\nu_{13}}{E_1} & \dfrac{-\nu_{13}}{E_1} & \dfrac{1}{E_3} & 0 & 0 & 0 \\[2ex] 0 & 0 & 0 & \dfrac{2(1+\nu_{12})}{E_1} & 0 & 0 \\[2ex] 0 & 0 & 0 & 0 & \dfrac{1}{G_{13}} & 0 \\[2ex] 0 & 0 & 0 & 0 & 0 & \dfrac{1}{G_{13}} \end{pmatrix} \quad (4)$$
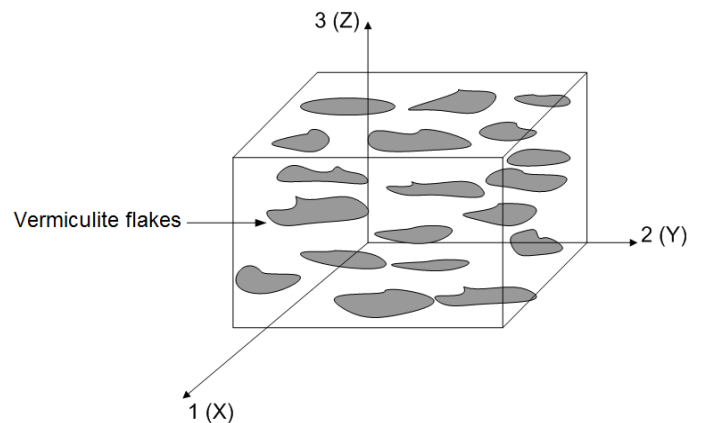

Fig. 4 Definition of the coordinate system

D. Procedure of compression test

Because of the brittle behavior of such materials, the samples were tested in compression. The uni-axial compressive stress–strain behaviors were performed by using an EPLEXOR® 500 testing machine at room temperature (20 °C) (Fig. 5). The tests were conducted under strain control, with a strain speed of 0.6 %/min. Five cycles were carried out for each sample, and the elastic modulus were the average (average values of five cycles) of the loaded and unloaded elastic modulus. Moreover, some tests were filmed with a camera PULNIX TM-4200 GE

(ability to capture 15 images per second). These images enable to track the strain evolution of the sample. The synchronization between the measures (force, displacement...) and saving images allows to provide an image for different loading states. About thirty samples were tested (10 of each series).
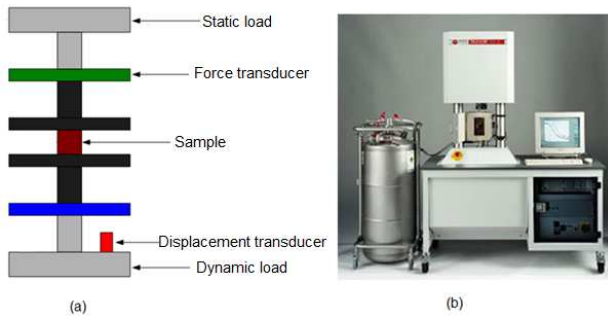

Fig. 5 EPLEXOR® 500 machine: scheme (a) and picture of EPLEXOR (b)

The capacity of the EPLEXOR® 500 machine is limited to 500 N, and to achieve the highest possible stress (higher to 80 MPa), it was necessary to reduce the surface of the loaded area. The cutting of these samples was carried out from cylindrical samples using a Leica RM2165 microtome (Fig. 6). This microtome allows:
- To obtain flat surfaces sample.
- To control the parallelism of the parallelepiped surfaces.
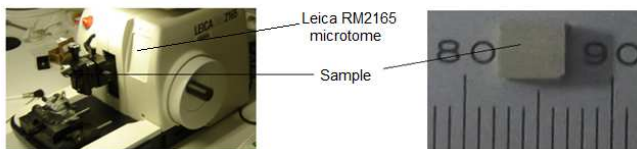- To control the sample dimensions.

Fig. 6 Sample cut with Leica RM2165 microtome

The samples have a parallelepiped shape, as shown in Fig. 7. The loading/unloading were performed in the transverse direction (along the 1 or 2 axis) and the longitudinal direction (according to the axis 3) of the samples. The axis 3 is the direction of compaction of the sample. The mechanical properties measured are: the longitudinal Young modulus, the transverse Young modulus, the Poisson coefficients and the elastic recovery of the samples.

III. EXPERIMENTAL RESULTS AND DISCUSSION

A. Micro-structure of compacted exfoliated vermiculite

First the microscopy observations show a good homogeneity of the micro structure. The pictures show a lamellar structure. The vermiculite flakes tend to aggregate into larger clusters. Moreover, the analysis of the SEM images highlights that porosity result from the lack of vermiculite flakes. Therefore these porosities have the shape of flakes. A measurement of the porosity using Mercury porosimetry allowed to evaluate the size of the porosity and porosity ratio [8]. These measures

were confirmed by the SEM images analysis using image processing software (ImageJ [17]). The mean value from Hg porosimetry is about 37% [8] (The value from image analysis is about 33%). It is important to underline that all porosities (connected and no connected porosities) have an effect on the mechanical behaviour of the studied porous media. It can be noticed that these porosities have an ellipsoid shape with average dimensions: $l_x \times l_y \times h$ =700±175 nm×700±175 nm×70±28 nm. The analyses of each SEM picture give some information on the orientation distribution of porosities. A simple measure of the orientation of each porosity shows that the orientation of these oblate porosities was mainly perpendicular to the axis of compaction. Measurement of the orientation of each porosity shows a Gaussian distribution around 0 ° compared to the compaction axis (see Fig. 8), with a full width at half maximum of 26 °. This value is less than that obtained by Balima [18](40 °) using small angle neutron scattering.
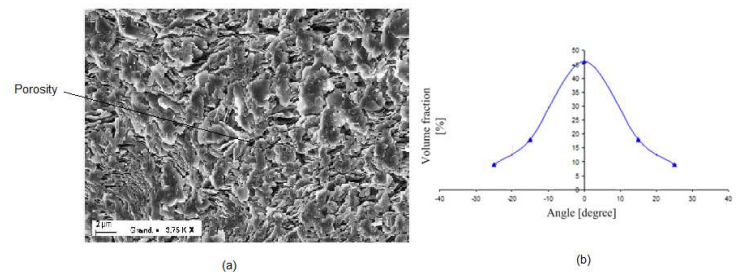

Fig. 7 (a) SEM micrographs of vermiculite flakes and (b) orientation distribution of porosities

B. Compressive properties of compacted exfoliated vermiculite

Fig. 9 shows a representative stress–strain curve of CEV samples. All curves exhibit a characteristic compressive behavior of porous materials. This behavior has three steps: the initiation of strain, the elastic stage, and a quasi-platform stage that appears. With a close look at the initial elastic stage, it can be noticed that CEV materials exhibit a nonlinear stress–strain behavior. The reason is that the strain consists of the flakes elastic strain and the 'structural strain', and these two types of coupled strain lead to a nonlinear behavior. On the other hand, loading/unloading cycles indicates significant stress–strain hysteresis, suggesting damping and energy absorption capacities.

The effects of vermiculite flakes, on the macroscopic behavior, are complex. Indeed, these flakes are oriented in any direction but with a Gaussian distribution, perpendicular to the compaction axis. So the flakes undergo compression, bending and torsion. It is obvious that the joints in this material play an important role in terms of the 'structure effect'. The macroscopic behavior may result from the friction between the flakes and/or from the irreversible flakes rearrangements.
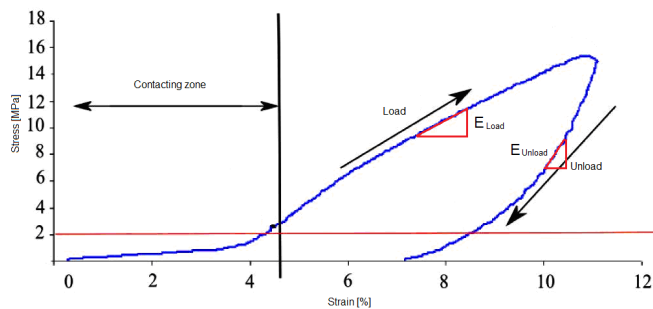
Fig. 8 Experimental curve of the load-unload test

Young modulus determination

Young's modulus is measured during loading/unloading test (see Fig. 8). Young's modulus is estimated from the slope of the loading or unloading curves. For a perfectly elastic material, it has the same slope as in loading and unloading configurations. The CEV materials have significantly different elastic modulus during loading and unloading. The slope of the linear part of the loading and unloading curve is taken as the loaded and unloaded elastic moduli, as shown on the Fig. 8. Both the loaded elastic modulus and unloaded elastic modulus would decrease as the porosity increases. The unloaded elastic modulus is noticeably greater than the loaded elastic modulus.

Table 2 resumes the Young's modulus values in loading and unloading in the longitudinal (axis of compaction: direction 3) and transverse direction (along the direction 1 and 2). The longitudinal modulus is greater than the transverse one. It has been verified that the mechanical behavior is the same for any direction in the transverse compaction plane. So, the samples are transversely isotropic. Indeed, the flakes of vermiculite are stacked on each others preferentially in the direction perpendicular axis to the compaction axis. This can be explained, first, by the transverse isotropic nature of vermiculite flakes, as shown in some studies [19]. It was found that the temperature of implementation significantly improves the Young's modulus of the VK. Longitudinal Young's modulus in the loading test is 250 MPa for VK20 and 485 MPa for VK200. For a temperature of implementation of 20 °C, the VL samples have a higher Young's modulus than the VK samples. Longitudinal Young's modulus in the loading is 450 MPa for VL20. Lithium exchange seems to improve the mechanical rigidity of CEV.

	Longitudinal Young's modulus [MPa]	transverse Young's modulus [MPa]
VK200 in loading	485±70	200±60
VK200 in unloading	1160±140	410±100
VL20 in loading	450±55	320±55
VL20 in unloading	1500±285	1060±155
VK20 in loading	250±40	230±20
VK20 in unloading	735±80	570±40

Table 2 Transverse and longitudinal Young modulus

In some studies [15, 16], measurements of mechanical properties were performed on the raw vermiculite with a flake sizes much larger than the studied CEV samples. Thus in [16], the values of Young's moduli of vermiculite (flake diameter between 4-8 mm) were measured: $E_L=19,9±4,03$ MPa and $E_T=1±0,26$ MPa. In [15], the measures are: $E_L=19,9±4,03$ MPa and $E_T=1±0,26$ MPa. For these two materials, the anisotropy is quite high, since the ratio $\dfrac{E_l}{E_t}$ is respectively about 20 and 30, while for studied CEV samples the ratios are between 1.3 and 2.8. The measurements in this study are performed on CEV whose size flakes is very small (grinding of raw vermiculite [8]). This difference can be explained by the very different flake size of vermiculite and related disorder in the stack. Grinding the sheets facilitates the densification and handling of samples. It is likely that compaction leads to a stiffening of the exfoliated vermiculite and a Young's modulus relatively high. It should be underline that the material used in this study is significantly different from the raw vermiculite. Indeed, the operations suffered by the vermiculite are numerous, chemical exfoliation, grinding, compaction ... This explains the large difference between the elastic modulus obtained in some studies [15, 16] and those obtained here.

Poisson coefficients Determination

For transversely isotropic material, there are two Poisson ratios to determine. The transverse and longitudinal strains were evaluated from images analysis (synchronized with the experimental measurements). The strain was evaluated with image analysis software (ImageJ [17]). A first step allows to validate this method by comparing the strain measure issues from the strain sensor and the strain measured using image analysis. The two types of measure provide similar values. The measure of the deformation with image analysis is thus validated. Each image corresponds to a given state of charge in the longitudinal direction or in the transverse direction, as shown in Fig. 9.
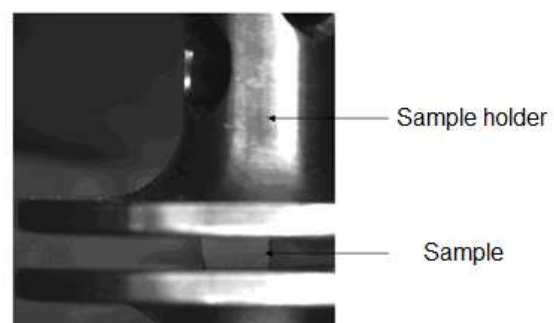

Fig. 9 Compression image of the vermiculite sample

The axis 3 is the isotropy axis, the two Poisson's ratios to be evaluated are: ν_{13} and ν_{12}. To determine these coefficients, two compression tests were performed:

- Compression in the longitudinal direction (3) and measuring of the transverse strain ε_{11} to evaluate the coefficient ν_{13}.
- Compression in the transverse direction (1 or 2) and measuring of the strain ε_{22} to evaluate the coefficient ν_{12}.

Poisson's ratios measurements were made for VK200 samples. Table 3 summarizes the mean values of Poisson's ratios.

Poisson ratio ν_{12}	Poisson ratio ν_{13}
0.11±0.01	0.31±0.02

Table 3 Poisson ratio values

In the literature, few Poisson's ratios measurements for vermiculite are presented. As the Young's modulus, Poisson's ratios depend on the type of vermiculite, the flakes size... Thus, in [15], Poisson's ratios measurements for raw vermiculite, with a flake size larger than the studied case, were made. The values found are: ν_{12}=0.03, ν_{13}=0.06 et ν_{31}=1.33. These values are very different from the measurements, but, as previously stated, the samples studied are very different from raw vermiculite.

Shear modulus determination

The shear modulus is determined by using the relationship of Saint Venant (1863):

$$\frac{1}{E_3} + \frac{1}{E_1} + \frac{2\nu_{13}}{E_1} = \frac{1}{G_{13}} \qquad (5)$$

As for the Poisson's ratio, the evaluation of the shear modulus is done for VK200 samples. The value obtained is: G_{13}=98±28 MPa.

Elastic recovery

For sealing application, the material must have a good elastic recovery. To determine this property, the thickness evolution during the compression test (loading/unloading) was measured. Fig. 10 illustrates a loading/unloading test curve and the specific parts used for the calculation of the elastic recovery.

According to ASTME-36, the elastic recovery r_e is defined with the following relation (6):

$$r_e = \frac{e_f - e_c}{e_i - e_c} \qquad (6)$$

e_i: initial thickness of the sample, e_c: thickness under maximum stress, e_f: final thickness after release of the load.

To minimize the measurement errors of elastic recovery, the initial and final thicknesses were measured for a stress of 2 MPa. This allows to start the measurement when the sample surfaces are in contact with the sample holder and not with few asperities (Cf Fig. 10).
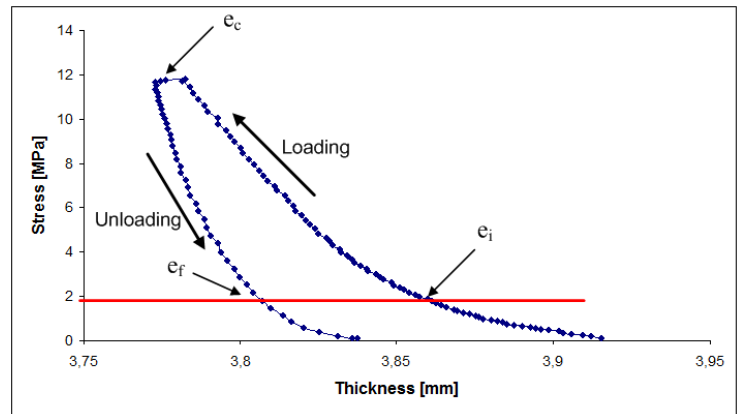

Fig. 10 Various quantities of a load/unload cycle to calculate elastic recovery

Table 4 summarizes the elastic recovery values in the longitudinal and transverse directions. The samples made with CEV have an excellent elastic recovery in the longitudinal direction (30% to 40%). The elastic recovery in the transverse direction is between 17% and 22%. In addition, it can be noticed that the type of vermiculite and implementation temperature does not affect the elastic recovery. The elastic recovery was also anisotropic with a factor about 2 between the longitudinal and transverse elastic recovery. Also, the elastic recovery in the longitudinal direction was the highest, which was interesting for the sealing application.

As comparison, the flexible graphite has an elastic recovery about 10%. The product "Thermiculite" [20-24] (Thermiculite is a vermiculite based material marketed for sealing applications) has an elastic recovery of 4.6% [25].

	Longitudinal direction	Transverse direction
VK200	38,6%	17,8%
VL20	36,7%	14%
VK20	40,8%	22,2%

Table 4 elastic recovery values

IV. CONCLUSION

This article presents a mechanical characterization of different samples of VEC: Potassium exchanged or lithium exchanged, exfoliated, grind and compacted with a pressure of 80 MPa at room temperature or 200 ° C. For low compression level, the mechanical behaviour of this material has two steps: *initial nonlinear deformation, strain-hardening 'pseudo-platform'*. In addition, for the cycles of loading and unloading, hysteresis phenomenon appears. Micro structure, characterized by SEM explains the transverse isotropic behaviour of this porous material. Moreover, the properties of the studied samples are very different from those of raw vermiculite. This difference can be explained by the microstructures of each media (flake sizes, orientation of flakes...).

Despite significant porosity volume ratio, this kind of material has interesting mechanical properties for applications such as sealing. Thus the elastic recovery has relatively large values

compared to other types of materials used for gaskets (carbon exfoliated and compacted). Finally, this article shows that implementation parameters impacts significantly on the mechanical behaviour of this type of material.

ACKNOWLEDGMENT

REFERENCES

[1] Sealing Technology," Vermiculite - the high temperature sealing material of the future?,"*Sealing Technology*,vol.46,1997, pp.8-9.

[2] Sealing Technology," Vermiculite gaskets to beat the heat "Sealing Technology,vol.1998,1998, pp.5.

[3] *Sealing Technology*," Production of vermiculite foil,"*Sealing Technology*,vol.2003,2003, pp.14.

[4] K. Carrado, F. Bergaya, Clay-based polymer Nanocomposites (CPN) CMS Workshop Lecture, The Clay Minerals Society, Chantilly, 2007.

[5] P. Podsiadlo, Z. Liu, D. Paterson, P. B. Mellersmith, N. A. Kotov," Fusion of seashell nacre and marine bioadhesive analogs: high-strength nanocomposite by layer-bylayer assembly of clay and L-3,4-dihydroxyphenylalanine polymer,"Advanced Materials,vol.19,2007, pp.949-955.

[6] Z. Tang, N. A. Kotov, S. Magonov, B. Ozturk," Nanostructured artificial nacre,"Nature Materials 2,2003, pp.413-418.

[7] N. Sheng, M. C. Boyce, D. M. Parks, G. C. Rutledge, J. I. Abes, R. E. Cohen," Multiscale micromechanical modelling of polymer/clay nanocomposites and the effective clay particle,"Polymer,vol.45,2004, pp.487-506.

[8] N. A. Nguyen, Elaboration et caractérisation de matériaux d'étanchéité à base de vermiculite, in: Université de Grenoble, 2012.

[9] N. van Garderen, F. J. Clemens, J. Kaufmann, M. Urbanek, M. Binkowski, T. Graule, C. G. Aneziris," Pore analyses of highly porous diatomite and clay based materials for fluidized bed reactors,"Microporous and Mesoporous Materials vol.0,2011.

[10] M. C. Sukop, H. Huang," Distribution of multiphase fluids in porous media: Comparison between lattice boltzmann modeling and micro-x-ray tomography,"Physical Review E - Statistical, Nonlinear, and Soft Matter Physics,vol.77,2008, pp.p. 026710.

[11] S. Sleutela, V. Cnuddeb, B. Masschaelec, J. Vlassenbroekc, M. Dierickc, L. Van Hoorebekec, P. Jacobsb, S. De Nevea," Comparison of different nano- and micro-focus X-ray computed tomography set-ups for the visualization of the soil microstructure and soil organic matter,"Computers & Geosciences,vol.34,2008, pp.931-938.

[12] M. F. M. Costa," Application of image processing to the charaterisation of nanostructures,"Revue of advanced material science,vol.6,2004, pp.12-20.

[13] K. Terzaghi," Theorical Soil Mechanics,"John Wiley and Sons Inc, Chicheister,1942.

[14] M. A. Biot," General theory of three-dimensional consolidation,"Journal of Applied Physics,vol.12,1941, pp.155-164.

[15] R. Goodall, Thermomechanical Properties of Highly Porous, Fire-Resistant Materials, Department of Materials Science and Metallurgy, University of Cambridge December 2003

[16] R. Goodall, C. Williams, J. A. Fernie, T. W. Clyne, Thermal Expansion and Stiffness Characteristics of a Highly Porous,Fire-Resistant Composite Material, in: ECCM 10, Brugge, Belgium, 2002.

[17] T. Ferreira, W. Rasband," ImageJ User Guide , ImageJ/Fiji 1.46,2012.

[18] F. Balima, Structure et porosité de systèmes lamellaires sous haute pression : cas du graphite et de la vermiculite, in: Université de Lyon, 2012.

[19] J. R. Hindman," Vermiculite,"Industrial Minerals and Rocks; Kogel, J.E., Trivedi, N.C., Barker, J.M. and Krukowski, S.T., Editors, Society for Mining, Metallurgy and Exploration Inc.,2006, pp.1015-1026.

[20] A. W. Atkinson, S. P. Bond, A. M. West , J. R. Hoyes," Gaskets,"Patent GB 2326201 A,1998.

[21] H. V. Dunn, Woolfenden, A. D. Thomas," A gaskets material and its process of production,"Patent WO 2006/075149 A1,2006.

[22] J. R. Hoyes, A. W. Atkinson, S. P. Bond, A. M. West " Gaskets,"Patent WO 98/53022,1998.

[23] J. R. Hoyes, A. W. Atkinson, S. P. Bond, A. M. West," Gaskets,"Patent US 6121360 A,2000.

[24] J. R. Hoyes, S. Woolfenden," Gaskets,"Patent US 7204492 B2,2007.

[25] F. Wiener, M. Bram, H. P. Buchkremer, S. Sebold," Chemical interaction between Crofer 22 APU and mica-based gaskets under simulated SOFC conditions,"J. Mater. Sci.,vol.42,2007, pp.2643-2651.